Electronic Supplementary Material (ESI) for Energy & Environmental Science.

Supporting Information

Pyrite FeS_2 for High-rate and Long-life Rechargeable Sodium Batteries

Zhe Hu, Zhiqiang Zhu, Fangyi Cheng, Kai Zhang, Jianbin Wang, Chengcheng Chen, Jun Chen*

Contents

Measurement of tapped density

20 g as-prepared FeS_2 microspheres and 20 g commercial bulk FeS_2 were put into the two glass tubes separately. By using JZ-7 tapped density analyzer, the tubes were shaken up and down for 10000 times. Then we measure the tapped volume of each sample in the tubes and calculate the tapping density by the following equation:

$$\text{Tapped density} = \frac{\text{Mass}}{\text{Tapped volume}}$$

The tapped volume of FeS_2 microspheres and commercial bulk FeS_2 is 9.1 cm^{-3} and 6.7 cm^{-3}, respectively. And the calculated tapping density is 2.2 g·cm^{-3} and 3.0 g·cm^{-3}, respectively.

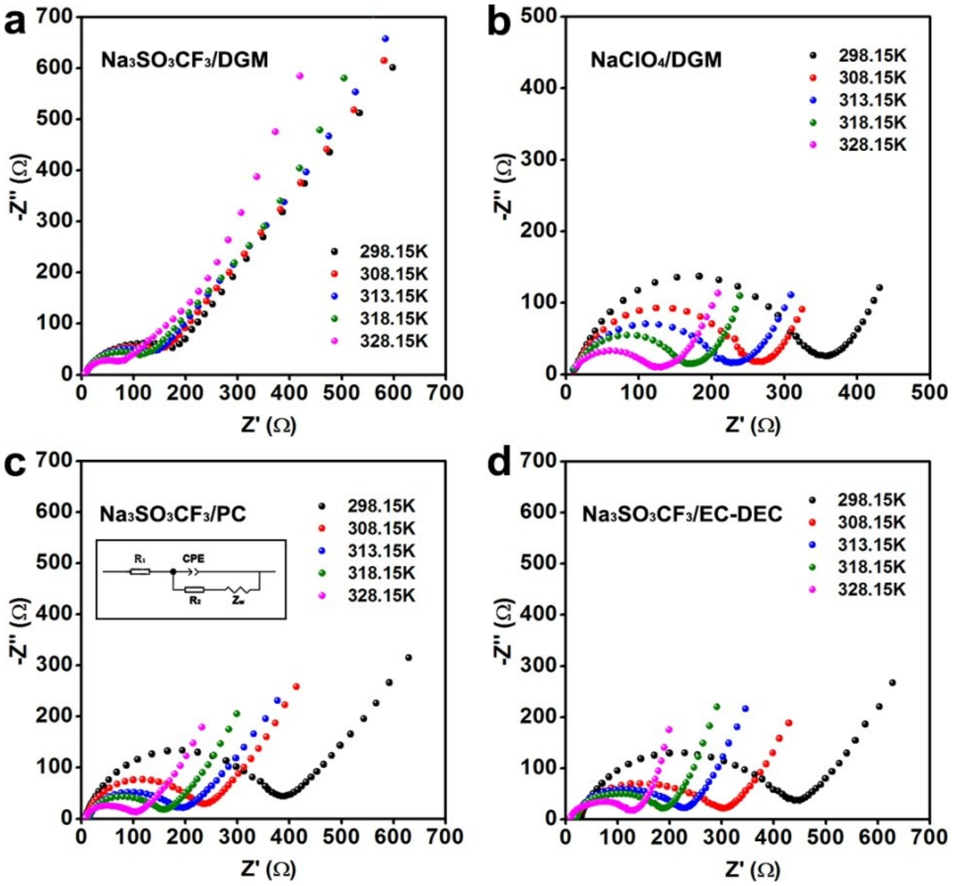

Fig. S1 The Nyquist plots of FeS_2-Na cell in **(a)** $NaSO_3CF_3$/DGM, **(b)** $NaClO_4$/DGM, **(c)** $NaSO_3CF_3$/PC, and **(d)** $NaSO_3CF_3$/EC-DEC. The equivalent circuit is put inside Fig.S1c.

The EIS characterization was taken under different temperature from 298.15 K to 328.15 K shown in the Fig.S1a-d. The plot features a compressed semicircle at high-frequency range and a line at low-frequency region, typical characteristics of combined charge transfer and electrolyte diffusion process. We can summarize that the Na-FeS_2 cell in the $NaSO_3CF_3$/DGM has the lowest R_{ct}. The other three kinds of electrolyte have larger R_{ct} at 25°C. We also calculated the activation energy (E_a) from the EIS data at different temperatures using the equations: $i_0=RT/nFR_{ct}$ (Equation S1) and $i_0=A\exp(-E_a/RT)$ (Equartion S2), where A is a temperature-independent coefficient, R is the gas constant, T is the absolute temperature, n is the number of transferred electrons, and F is the Faraday constant.[1, 2] $NaSO_3CF_3$/DGM shows the lowest E_a, which means that e^- transport easier in the cathode material with $NaSO_3CF_3$/DGM than the other three electrolytes.

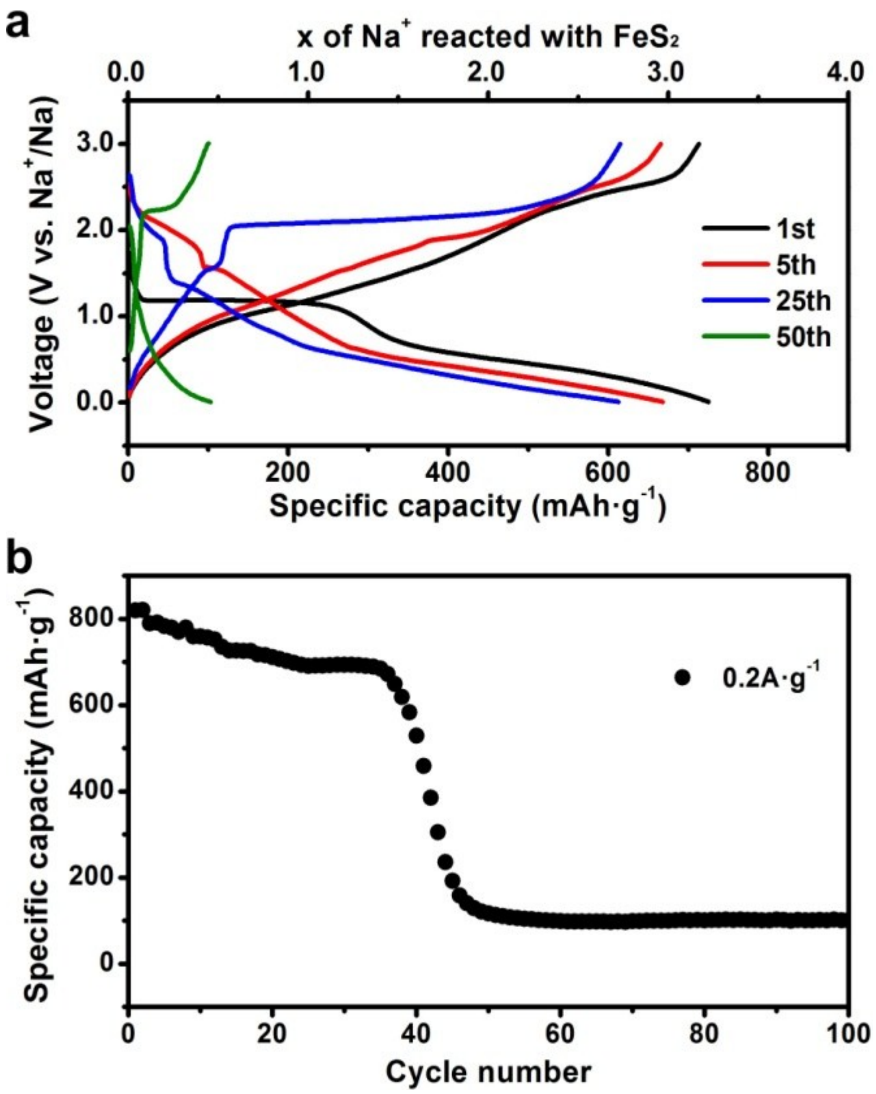

Fig. S2 (a) Typical charge/discharge curves and **(b)** cyclic property of FeS_2 electrode in $NaSO_3CF_3$/DGM in the voltage range of 0.1−3.0 V at 0.2 $A\cdot g^{-1}$.

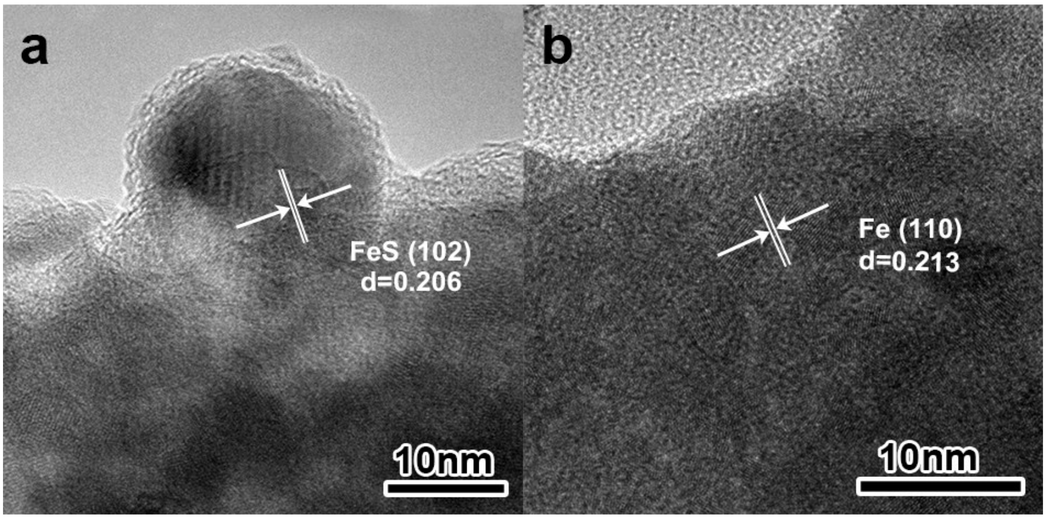

Fig. S3 HRTEM images of the cathode material in the FeS_2/Na battery at **(a)** 0.5 V and **(b)** at 0.1 V at 1st cycle. Fig. S3a and S3b show the HRTEM images of the cell discharging to 0.5 V and 0.1 V, and the most reliable intermediates are FeS and Fe according to the visible crystal fringe. However the other production sodium sulfide is not clearly found in the HRTEM. The low crystallization of the sodium sulfides may exist.[3]

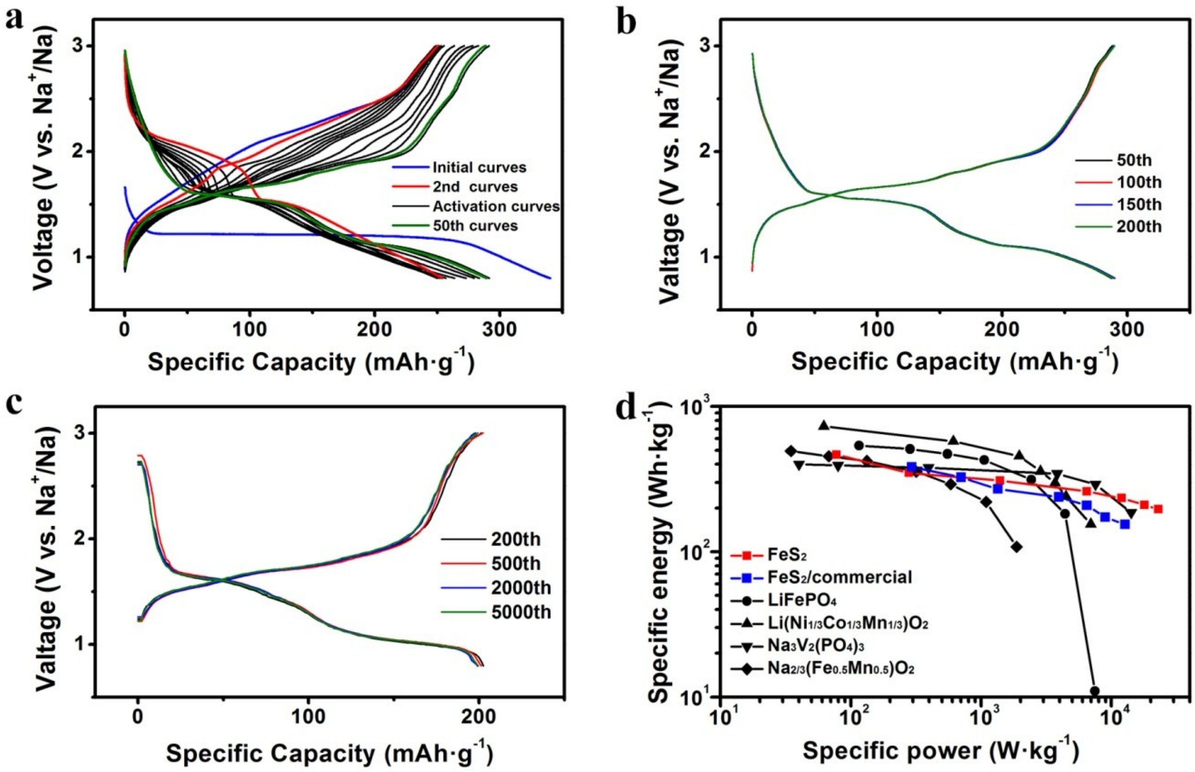

Fig. S4 The charge and discharge curves **(a)** from the 1st to 50th cycle and **(b)** from 50th to 200th at 0.1 A·g^{-1}, and **(c)** from 200th to 5000th at 1 A·g^{-1}. **(d)** Ragone plots of prepared and commercial FeS_2 and other typical Li/Na-host materials.

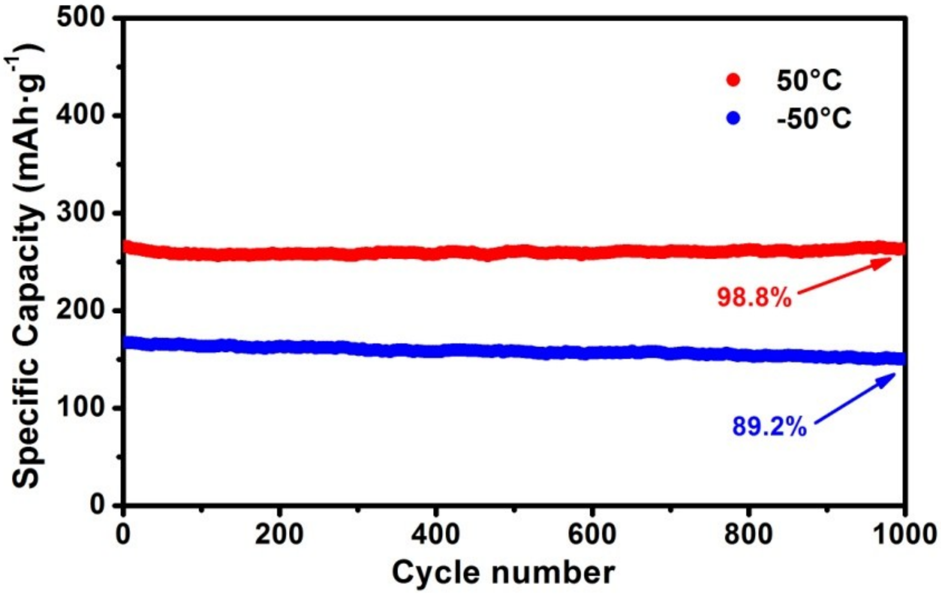

Fig. S5. Cyclic performance of FeS_2 microspheres at −50°C and 50 °C at 1 A·g^{-1}. (The capacity retention is signed inset the image)

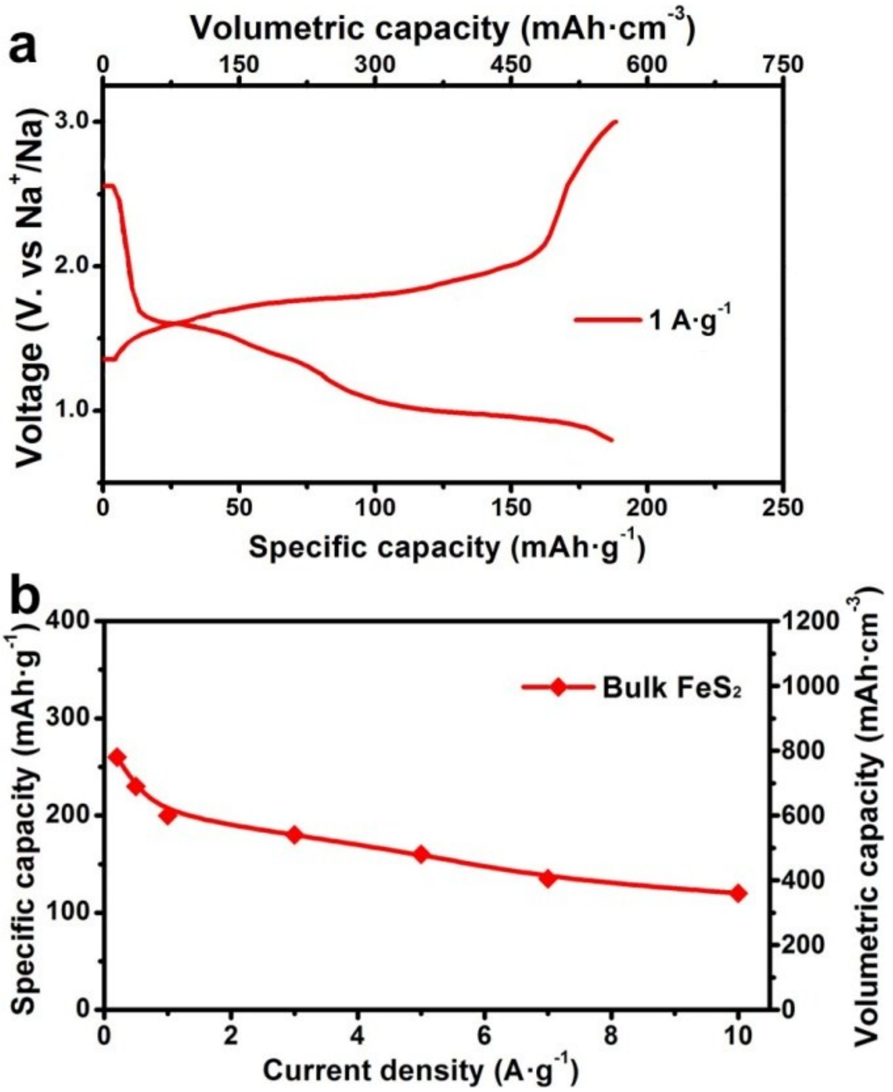

Fig. S6 (a) Typical discharge/charge curves and **(b)** rate performance of Na-FeS$_2$ battery with commercial bulk FeS$_2$.

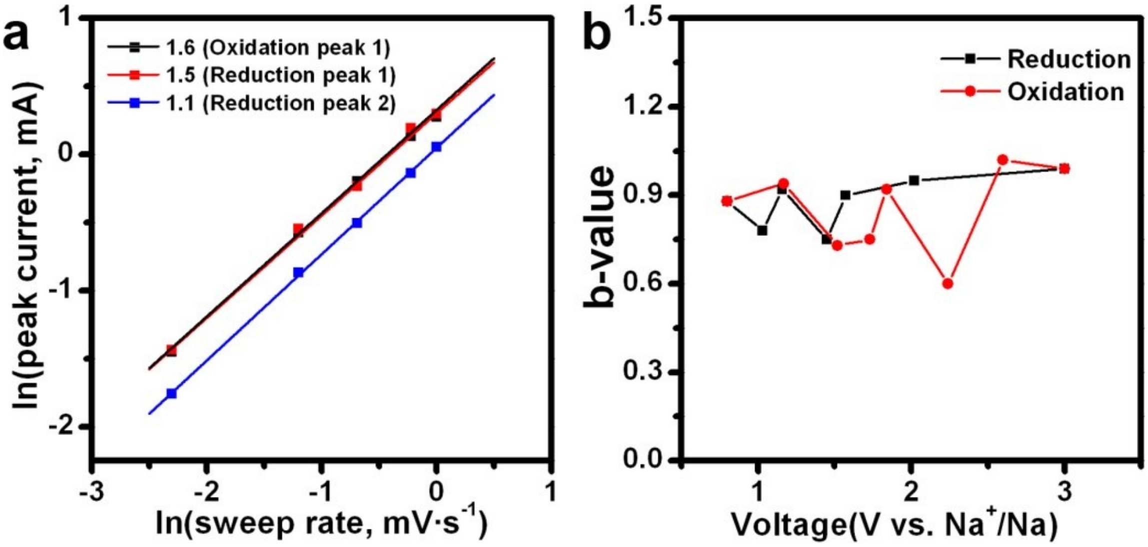

Fig. S7 (a) The fitted lines and ln(peak current) versus ln(v) for separating the diffusion-controlled capacity and capacitive-controlled capacity. **(b)** b-value at different oxidation/reduction states. We have calculated the capacitance contribution by using the relation $i = av^b$ (Equation S3) and $\ln i = b\ln v+\ln a$ (Equation S4), where i is the peak current, v is potential sweep rate, and a, b are adjustable values.[4] When b-value approaches to 1, the system is mainly controlled by capacitance; while b-value is closed to 0.5, the Na^+ insertion process dominates. We read the current density i at different peaks at different sweep rates from the CV curves (Fig. 4c) and used Eq. S2 to simulate the already known value of $\ln i$ and corresponding $\ln v$. The slope of the lines in Fig. S7a is just the b value, and detailed value is summarized in the Fig. S7b. As the average b value is ~0.7, we confirm that the capacitance contribution cannot be neglected. Moreover the read value i is consisted of two parts, the mechanisms of the capacitive effect (k_1v) and diffusion-controlled insertion ($k_2v^{1/2}$). Because the k_1 and k_2 are fixed for the same electrochemical reaction, so we the peak current of the same voltage position at different sweep rates to calculate the k_1 and k_2 using the equation $i = k_1v + k_2v^{1/2}$ (Equation S5). Then the capacitance contribution was depicted in Fig. 4d.

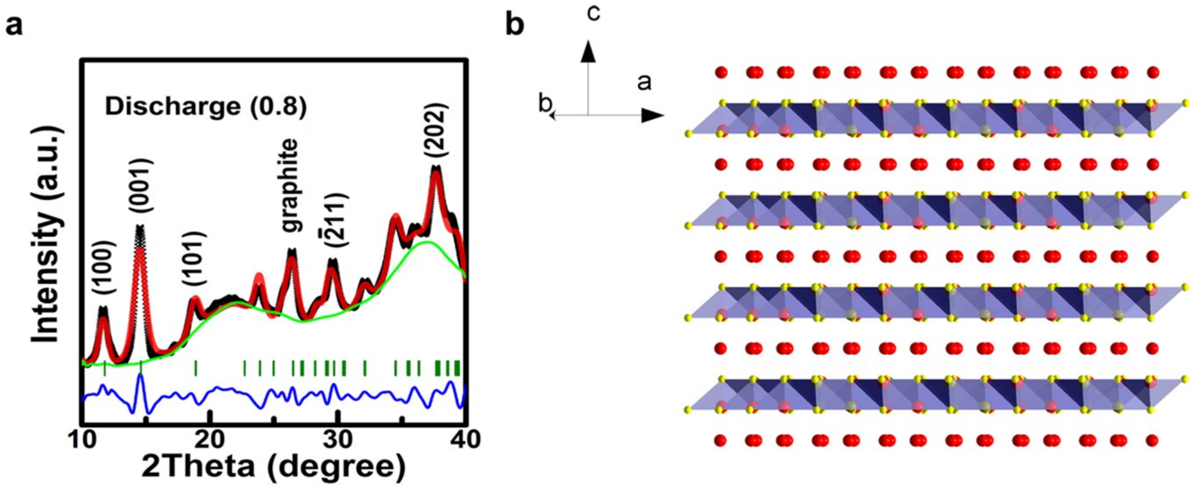

Fig. S8 (a) Rietveld refinement and **(b)** illustrative crystal structures of the Na_xFeS_2 cathode material at 0.8 V. Red spheres: Na ions; yellow spheres: sulfide; purple tetrahedron: Fe-S layers. Rietveld refinement was carried out by using the GSAS software.[5, 6] The result shows that the product belong to trigonal system and the residual factor (R_{wp}=0.0577 and R_p=0.0509) indicated that the refined XRD pattern fitted well with the experimental data, giving calculated cell parameters of *a*=8.59 Å, *b*=3.59 Å, and *c*=5.97 Å (C=120°).

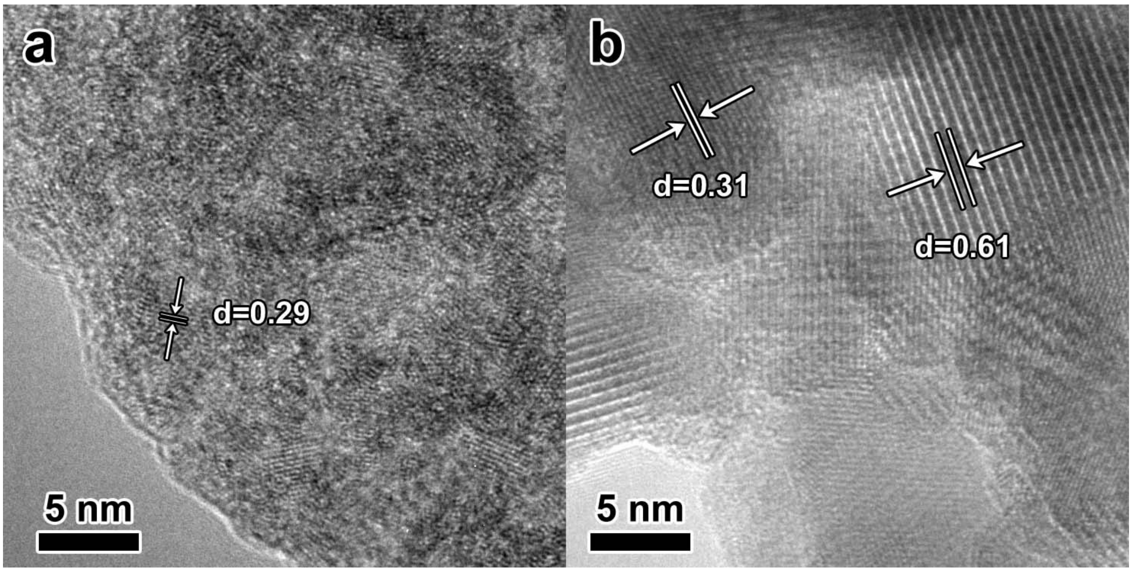

Fig. S9 HRTEM images of the electrode at IV and IX (the label coming from Fig. 5a)

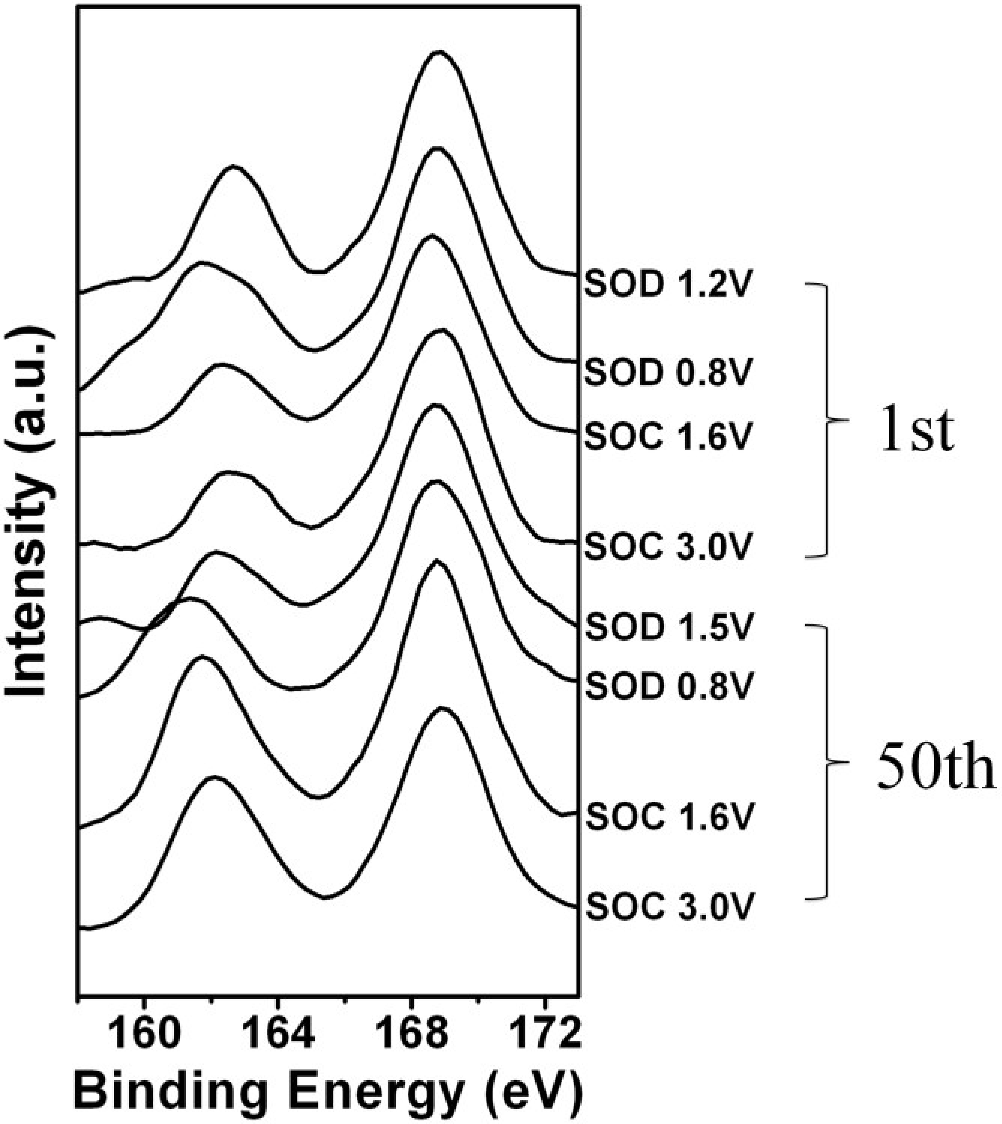

Fig. S10 The XPS data of the S $2p_{3/2}$ collected at different charge and discharge voltages at the first cycle and the 50th cycle. Fig. S10 shows the XPS data of S $2p_{3/2}$. The peaks around 168.5 eV are attributed to the S^{6+} in $NaCF_3SO_3$. And obviously changing happens to the peak at ~162 eV. At both the 1st and 50th cycle, when the cell is discharging to 0.8 V, the peak shift to a low binding energy indicating the tendency for S_2^{2-} turning into S^{2-}. When it comes to the charging process, the peak shifts to the higher binding energy, which means a reversible transformation of the two types of S during cycles.

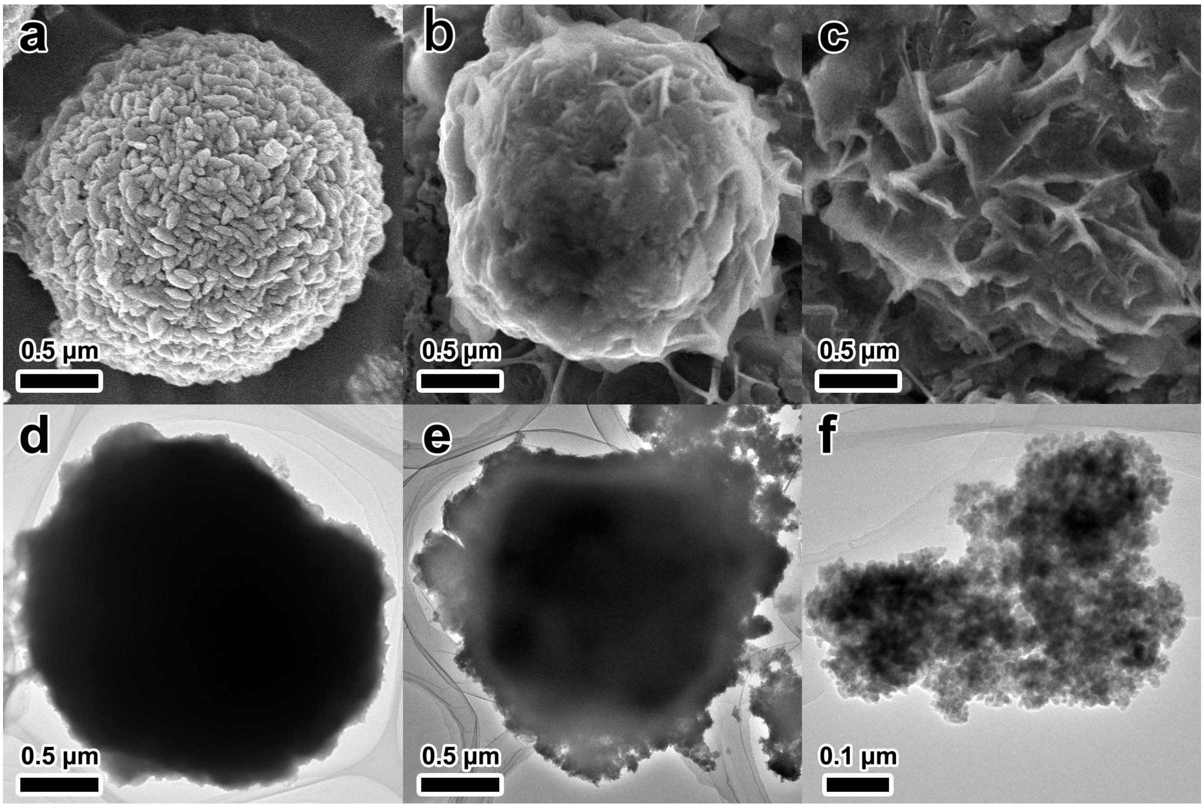

Fig. S11 The SEM and TEM images of the electrode matierials: **(a,d)** pure FeS_2 microspheres, **(b,e)** after cycling 50 times at 0.8 V, and **(c,f)** after cycling 20000 times at 0.8 V.

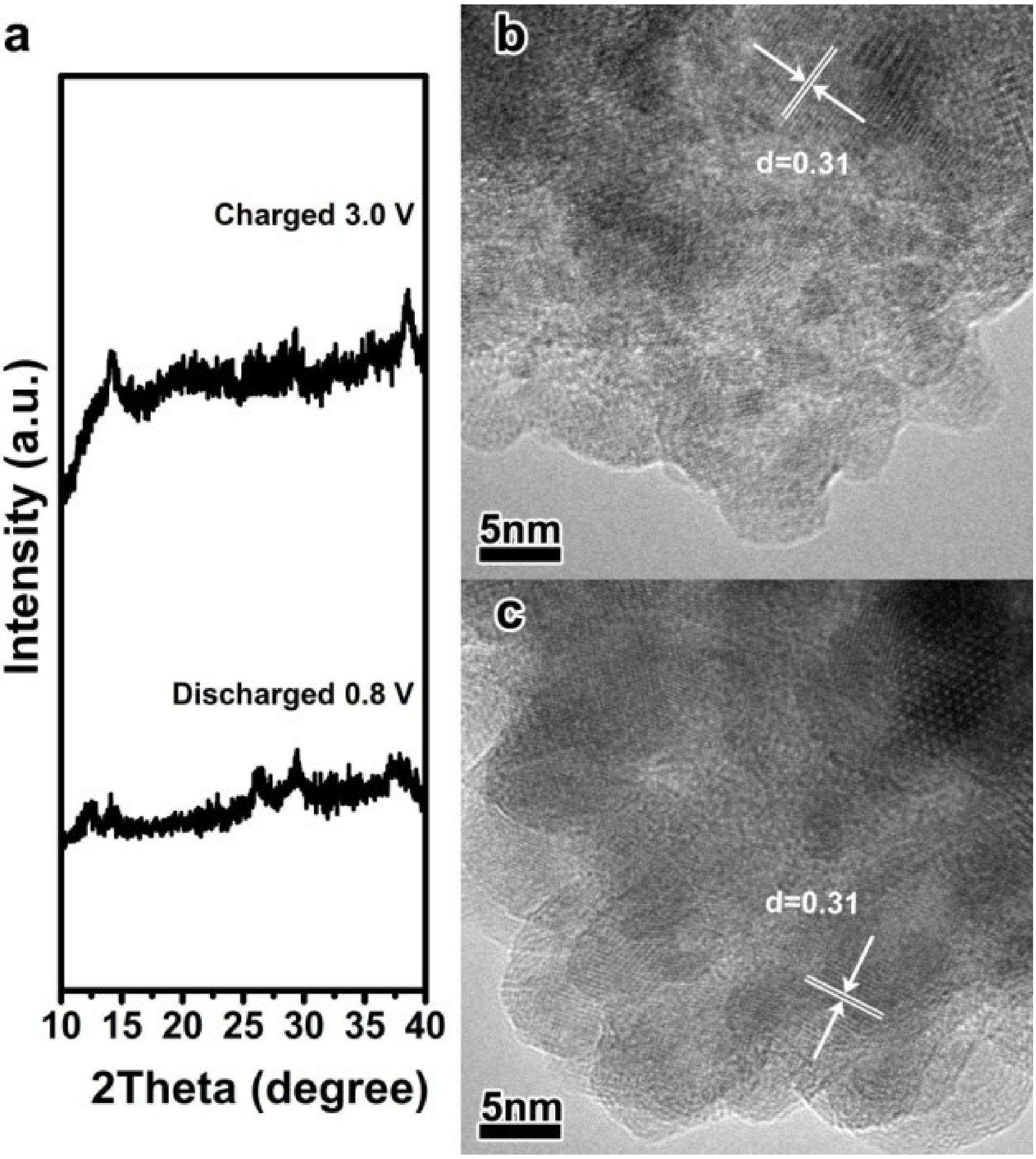

Fig. S12 (a) The XRD data of electrode materials at 3.0 V and 0.8 V after cycling 20000 times. HRTEM images of the cathode materials in Na/FeS_2 batteries at **(b)** 3.0 V and **(c)** 0.8 V.

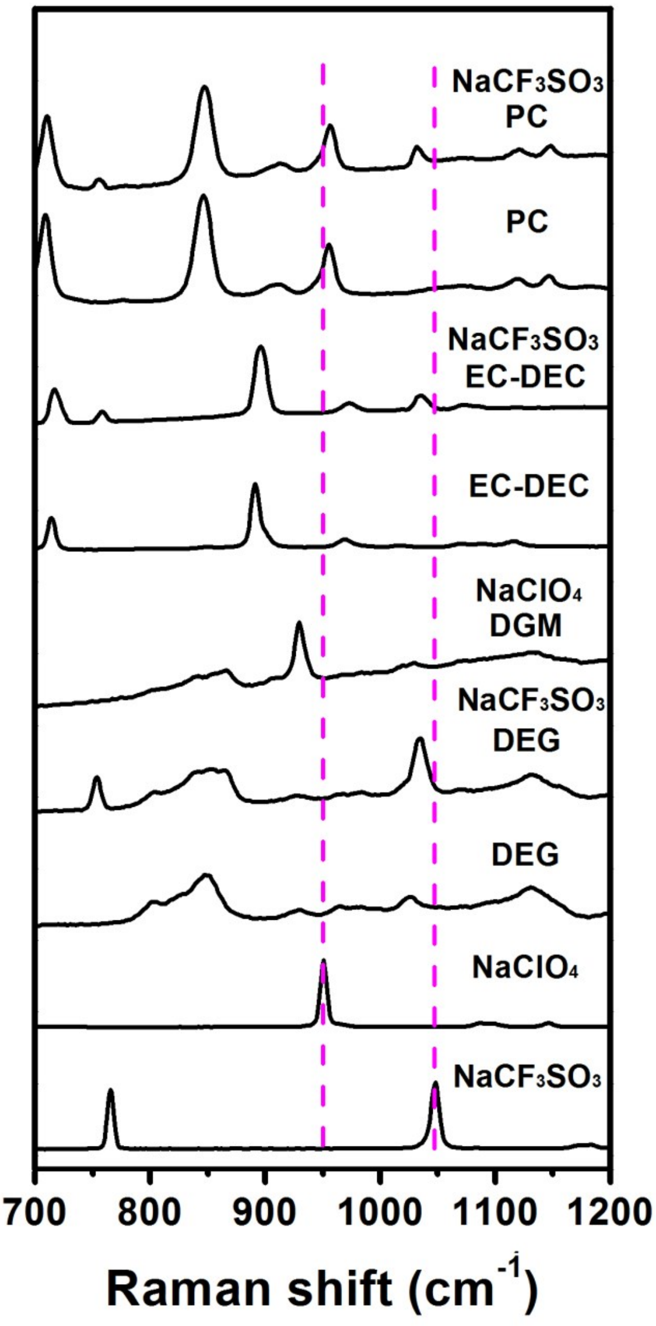

Fig. S13 Raman spectra of different kinds of solvent, salt, and solvent-salt mixture.

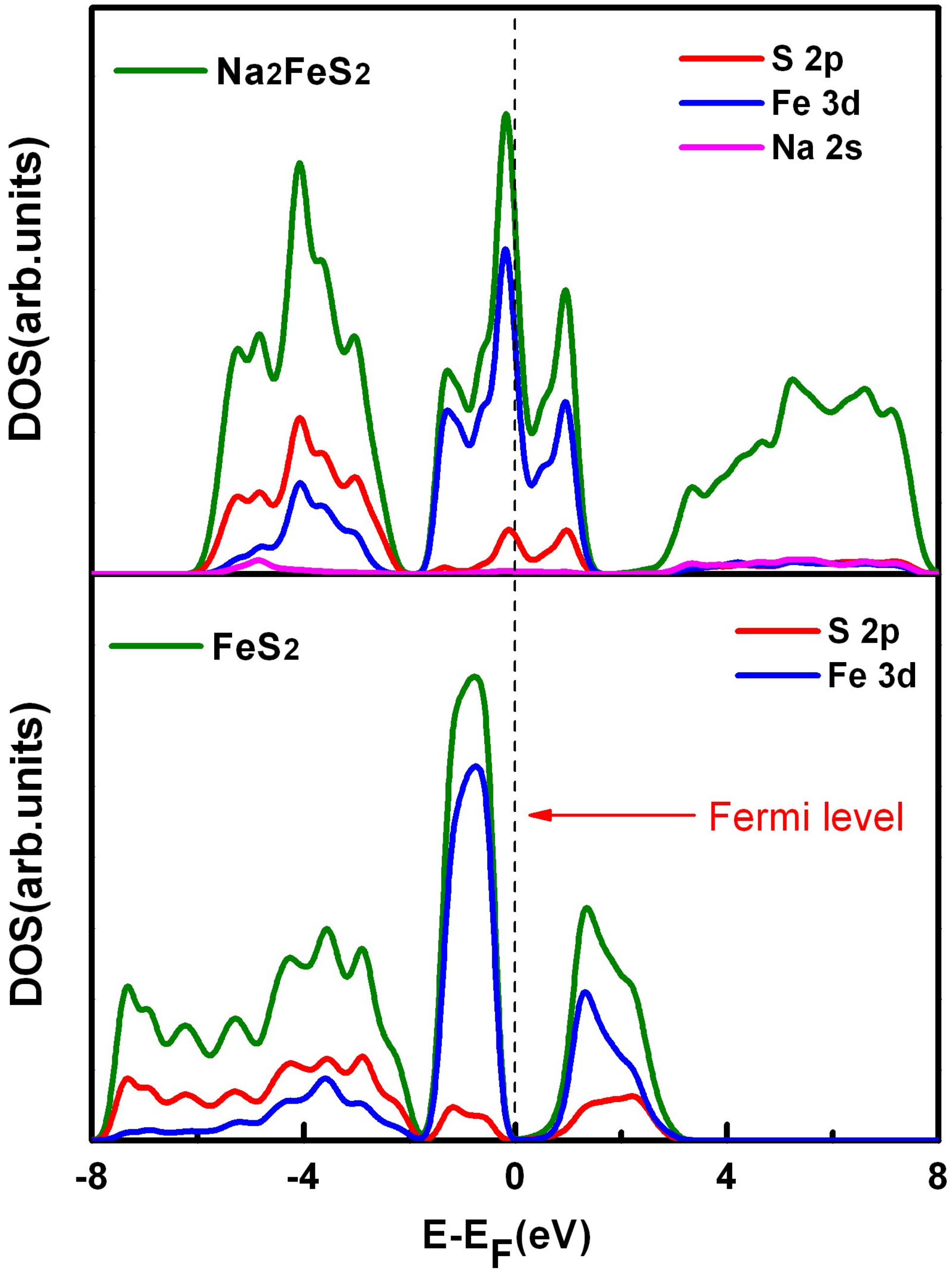

Fig. S14 The total and partial density of states of Na_2FeS_2 (up) and FeS_2 (down). The dot line represents the Fermi level.

Computational Details

Density Function Theory (DFT) calculation was performed by the Vienna ab initio simulation package (VASP).[7] The projector-augmented wave Method (PAW) was adopted to describe the ion-electron interaction.[8] We applied the generalized gradient approximation (GGA) to approximate exchange-correlation potential with the function of Perdew and Wang (PW91).[9] A cutoff energy of 360 eV was used. A unit cell of FeS_2 and supercell (2 × 1 × 1) of Na_2FeS_2 were constructed. For structure optimizations, convergence criterions of the electronic and ionic interation were 10^{-5} eV and 10^{-2} eV/Å, respectively. The Brillouin zone was sampled by Monkhorst-Pack k points mesh of 7 × 7 × 7 and 3 × 3 × 7 for FeS_2 and Na_2FeS_2, respectively [Na_2FeS_2 was built by optimizing the Li_2FeS_2 structure (JCPDS Card No. 80-578)]. For electronic structure calculations, larger grids of 14 × 14 × 14 and 6 × 6 × 14 were adopted for FeS_2 and Na_2FeS_2, respectively.

Fig. S14 illustrates the total density of states (TDOS) of Na_2FeS_2 and FeS_2. The TDOS of FeS_2 reveals clear gap near the Fermi level and indicates the semiconductive nature of FeS_2, agreeing with previous simulations.[10] In contrast to FeS_2, there are obvious states in the Fermi level of Na_2FeS_2, suggesting metallic property and enhanced electrical conductivity. The metallic property can be attributed to the p orbitals of S atoms and d orbitals of Fe atoms. In addition, the s orbitals of Na atoms overlap with that of p orbitals of S atoms and d orbitals of Fe atoms, indicative of interaction between Na, Fe, and S. The implied good electron conductivity of Na_2FeS_2 is another important factor responsible for the good rate performance of discharged pyrite electrode.

References:

1. H. Ma, S. Zhang, W. Ji, Z. Tao and J. Chen, *J. Am. Chem. Soc.*, 2008, **130**, 5361.
2. H. Gao, Z. Hu, K. Zhang, F. Cheng and J. Chen, *Chem. Commun.*, 2013, **49**, 3040.
3. C. Zhu, X. Mu, P. A. van Aken, Y. Yu and J. Maier, *Angew. Chem. Int. Ed.*, 2014, **53**, 2152.
4. T. Brezesinski, J. Wang, S. H. Tolbert and B. Dunn, *Nat. Mater.*, 2010, **9**, 146.

5. A.C.Larson and R. B. V. Dreele, *"General Structure Analysis System (GSAS)", Los Alamos National Laboratory Report LAUR.* , 1994, 86.
6. B. H. Toby, *J. Appl. Crystallogr.*, 2001, **34**, 210.
7. G. Kresse and J. Hafner, *Phys. Rev. B*, 1993, **47**, 558.
8. P. E. Blöchl, *Phys. Rev. B*, 1994, **50**, 17953.
9. J. P. Perdew, J. A. Chevary, S. H. Vosko, K. A. Jackson, M. R. Pederson, D. J. Singh and C. Fiolhais, *Phys. Rev. B*, 1992, **46**, 6671.
10. Y. Yamaguchi, T. Takeuchi, H. Sakaebe, H. Kageyama, H. Senoh, T. Sakai and K. Tatsumi, *J. Electrochem. Soc.*, 2010, **157**, A630.